VISION
RESEARCH

An International Journal for Functional Aspects of Vision

SPECIAL ISSUE
RETINAL DEGENERATION AND GENE THERAPY

GUEST EDITOR
WOLFGANG BAEHR
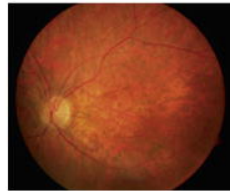
Biochemistry & Cell Biology • Molecular Biology & Genetics
Anatomy, Physiology, Pathology & Pharmacology • Optics, Accommodation & Refractive Error
Circuitry & Pathways • Psychophysics • Perception • Attention & Cognition
Computational Vision • Eye Movements & Visuomotor Control

This article was published in an Elsevier journal. The attached copy is furnished to the author for non-commercial research and education use, including for instruction at the author's institution, sharing with colleagues and providing to institution administration.

Other uses, including reproduction and distribution, or selling or licensing copies, or posting to personal, institutional or third party websites are prohibited.

In most cases authors are permitted to post their version of the article (e.g. in Word or Tex form) to their personal website or institutional repository. Authors requiring further information regarding Elsevier's archiving and manuscript policies are encouraged to visit:

http://www.elsevier.com/copyright

SANS (USH1G) expression in developing and mature mammalian retina

Nora Overlack [1], Tina Maerker [1], Martin Latz, Kerstin Nagel-Wolfrum, Uwe Wolfrum *

Department of Cell and Matrix Biology, Institute of Zoology, Johannes Gutenberg-University of Mainz, Germany

Abstract

The human Usher syndrome (USH) is the most common form of combined deaf-blindness. Usher type I (USH1), the most severe form, is characterized by profound congenital deafness, constant vestibular dysfunction and prepubertal-onset of retinitis pigmentosa. Five corresponding genes of the six USH1 genes have been cloned so far. The USH1G gene encodes the SANS (scaffold protein containing ankyrin repeats and SAM domain) protein which consists of protein motifs known to mediate protein–protein interactions. Recent studies indicated SANS function as a scaffold protein in the protein interactome related to USH.

Here, we generated specific antibodies for SANS protein expression analyses. Our study revealed SANS protein expression in NIH3T3 fibroblasts, murine tissues containing ciliated cells and in mature and developing mammalian retinas. In mature retinas, SANS was localized in inner and outer plexiform retinal layers, and in the photoreceptor cell layer. Subcellular fractionations, tangential cryosections and immunocytochemistry revealed SANS in synaptic terminals, cell–cell adhesions of the outer limiting membrane and ciliary apparati of photoreceptor cells. Analyses of postnatal developmental stages of murine retinas demonstrated SANS localization in differentiating ciliary apparati and in fully developed cilia, synapses, and cell–cell adhesions of photoreceptor cells.

Present data provide evidence that SANS functions as a scaffold protein in USH protein networks during ciliogenesis, at the mature ciliary apparatus, the ribbon synapse and the cell–cell adhesion of mammalian photoreceptor cells. Defects of SANS may cause dysfunction of the entire network leading to retinal degeneration, the ocular symptom characteristic for USH patients.
© 2007 Elsevier Ltd. All rights reserved.

Keywords: Usher syndrome; Photoreceptor cells; Connecting cilium; Synapse; Ciliogenesis; Retinal development

1. Introduction

The human Usher syndrome (USH) is the most frequent cause of combined hereditary deaf-blindness. USH is genetically heterogeneous with at least 12 chromosomal loci involved (Ebermann et al., 2007; Reiners, Nagel-Wolfrum, Jurgens, Marker, & Wolfrum, 2006). Depending on the degree of clinical symptoms, USH can be divided into three types USH1, USH2, and USH3 (Ahmed, Riazuddin, Riazuddin, & Wilcox, 2003; Davenport & Omenn, 1977; Petit, 2001). USH1 represents the most severe form, characterized by profound congenital deafness, constant vestibular dysfunction and prepubertal-onset of retinitis pigmentosa (RP) (Kremer, van Wijk, Märker, Wolfrum, & Roepman, 2006; Reiners et al., 2006).

The gene products of the nine identified USH genes are assigned to various protein classes and families as recently reviewed in Reiners et al. (2006) and Kremer et al. (2006): USH1B encodes for the molecular motor myosin VIIa. Harmonin (USH1C), SANS (scaffold protein containing ankyrin repeats and SAM domain, USH1G) and whirlin, more recently identified as USH2D (Ebermann et al., 2007) belong to the group of scaffold proteins. Cadherin 23 (USH1D) and protocadherin 15 (USH1F) represent cell–cell adhesion proteins, whereas USH2A and USH2C

* Corresponding author. Address: Johannes Gutenberg-Universität, Institut für Zoologie, D-55099 Mainz, Germany. Fax: +49 6131 39 23815.
E-mail address: wolfrum@uni-mainz.de (U. Wolfrum).
[1] These authors contributed equally to this work.

encode for the large transmembrane proteins, the USH2A isoform b and the very large G protein coupled receptor 1b (VLGR1b). The four-transmembrane-domain protein clarin-1 (USH3A) is so far the only identified member of USH3.

Previous analyses elucidated the assembly of all USH1 and USH2 proteins into an USH protein network mediated by the USH1C gene product—the scaffold protein harmonin (Adato et al., 2005; Boeda et al., 2002; Reiners, Marker, Jurgens, Reidel, & Wolfrum, 2005; Reiners et al., 2003, Reiners, van Wijk, et al., 2005; Siemens et al., 2002; Weil et al., 2003). Since all proteins of the network were found at the synapse of photoreceptor cells, a role of this network in maintaining synaptic integrity was proposed (Reiners, van Wijk, et al., 2005). In inner ear hair cells the USH protein network is involved in the development of stereocilia and in signal transduction (Adato et al., 2005; Boeda et al., 2002; Kremer et al., 2006). Lately, the scaffold protein SANS came into focus of interest to mediate further protein complexes (Adato et al., 2005). Most recent work identified SANS as an organizer of a harmonin independent USH protein network at the ciliary apparatus of vertebrate photoreceptor cells (Maerker et al., 2007).

The USH1G gene product SANS is composed of different domains (Fig. 1a) capable of mediating protein-protein interactions (Nourry, Grant, & Borg, 2003; Sedgwick & Smerdon, 1999; Stapleton, Balan, Pawson, & Sicheri, 1999; Weil et al., 2003). Three N-terminal ankyrin repeats are followed by a central domain, a SAM (sterile alpha motif) domain and a class I PBM (PDZ-binding motif) at the C-terminus. The central domain is interacting with both MyTH4 (myosin tail homology 4) and FERM (4.1, ezrin, radixin, moesin) domains of myosin VIIa and mediates SANS homodimerization. The SAM domain interacts with harmonin PDZ1 and PDZ3 (Adato et al., 2005), whereas the C-terminus of SANS containing the SAM domain and the PBM class I interact with whirlin PDZ1 and PDZ2 (van Wijk et al., 2006) (Fig. 1b).

So far, the SANS protein expression and its function was predominantly studied in inner ear hair cells. Analyses in SANS deficient *jackson shaker* mice revealed disorganized stereocilia bundles in the hair cells of the cochlea (Kikkawa et al., 2003). Further studies elucidated SANS localization in the apical part and the synapses of outer and inner hair cells as well as in the basal body of outer hair cells (Adato et al., 2005). Due to the latter localization pattern SANS was proposed as an important component for proper development of hair cells. Since the SANS protein expression was still elusive, the present study was performed to analyze the localization of SANS during retinal development and its subcellular distribution in mature retina.

Here, we show that SANS is not only expressed in the cochlea, but also in other tissues containing ciliated cells, as the retina, the brain, the lung, the testis, and the olfactory epithelium. Immunohistochemistry of adult murine retina indicated SANS localization in the inner plexiform layer and outer plexiform layer, as well as in the photoreceptor cell layer. The subcellular expression of SANS was further analyzed by different independent methods revealing SANS expression at the ciliary complex and at the synapse of photoreceptor cells. During postnatal development of the retina SANS was localized in basal bodies and maturing cilia of photoreceptor cells. Present data provide evidence that the SANS protein functions as an integral component of USH protein networks in diverse compartments of photoreceptor cells.
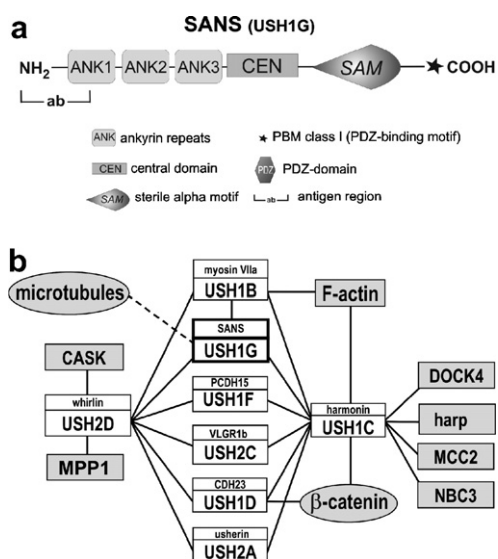
Fig. 1. Domain structure of the USH1G protein SANS and simplified scheme of the protein interactome related to human Usher syndrome. (a) SANS (Scaffold protein containing ankyrin repeats and SAM domain) consists of three N-terminal ankyrin repeats (ANK1-3), a central domain (CEN) and a C-terminal SAM (sterile alpha motif) domain. The last three amino acids comprise a PBM class I (PDZ-binding motif I) indicated by an asterisk. The region chosen for antibody generation is accentuated. (b) Scheme of a simplified version of the Usher protein interactome in relation to SANS. Interaction partners of the USH scaffold proteins harmonin, SANS and whirlin were described in detail in Kremer et al. (2006). Recently, whirlin was identified as USH2D (Ebermann et al., 2007) and its binding to MPP1 was more recently shown (Gosens et al., 2007). On the basis of simplification several protein-protein interactions are not shown. Confirmed interaction partners are indicated by solid lines, putative associations by dotted lines.

2. Methods

2.1. Animals and tissue preparation

All experiments described herein conform to the statement by the Association for Research in Vision and Ophthalmology (ARVO) as to care and use of animals in research. Adult C57BL/6J mice, Wistar Kyoto albino rats and *Xenopus laevis* were maintained under a 12 h light–dark cycle, with food and water *ad libitum*. After sacrifice of the animals in CO_2 (rodents) or chloroform (*Xenopus*) and decapitation, subsequently entire eyeballs were dissected or retinas were removed through a slit in the cornea prior to further analysis. For Western blot analyses, appropriate tissues were homogenized in modified RIPA buffer (10 mM Tris, 1 mM $CaCl_2$, 0.5% NP-40, 0.5% desoxycholinacid, 0.1% SDS, 150 mM NaCl,

10 mM NaF, 20 mM β-glycerolphosphate, pH 7.4) containing a protease inhibitor cocktail (Roche Diagnostics, Mannheim, Germany). Pig and bovine eyeballs were obtained from the local slaughterhouse.

2.2. Antibodies

Polyclonal antibodies to SANS were generated in rabbits against a recombinant expressed murine SANS fragment (amino acids 1–46). Expression of the fusion proteins and the purification of antibodies were performed as described elsewhere (Reiners et al., 2003). Antibodies against acetylated α-tubulin, γ-tubulin, actin, and PSD-95 (clone 7E3-1B8) were acquired from Sigma–Aldrich (Deisenhofen, Germany). Anti-cytochrome c antibodies (COX IV) were purchased from Invitrogen (Karlsruhe, Germany), anti-synaptophysin (SVP38), and anti-β-catenin antibodies were obtained from Santa Cruz Biotechnology (Santa Cruz, USA). Monoclonal antibodies against centrins (clone 20H5, detecting all four centrin isoforms) and opsin (clone K16-155) were previously described (Adamus, Arendt, Zam, McDowell, & Hargrave, 1988; Adamus, Zans, Arendt, Palczewski, McDowell, & Hargrave, 1991; Wolfrum & Salisbury, 1998; Wolfrum & Schmitt, 2000). Secondary antibodies were purchased from Invitrogen, Sigma–Aldrich or Rockland (Gilbertsville, USA). Preadsorption of anti-SANS antibodies was performed by incubation of antibodies for 1–2 h at room temperature with 1 mg/ml of the specific antigen used for immunization. After short centrifugation preadsorbed antibodies were applied to the retina cryosection or Western blot membrane in the appropriate dilution, and were treated like others.

2.3. Isolation of ROS

Rod outer segments (ROS) were purified from bovine retinas using the discontinuous sucrose gradient method as previously described (Papermaster, 1982; Pulvermüller et al., 2002). Since immunofluorescence microscopy showed no differences between dark and light adaptation, the procedure was performed under light. The purity of ROS was confirmed by Western blot analyses. Briefly, retinas were vortexed in 1.4 ml homogenizing medium (1 M sucrose, 65 mM NaCl, 0.2 mM MgCl$_2$, 5 mM Tris–acetate, pH 7.4) and centrifuged at 2000g for 4 min at 4 °C. The supernatant was diluted with twice of its volume in 0.01 M Tris–acetate, pH 7.4, and gently mixed. ROS were pelleted at 2000g for 4 min at 4 °C and resuspended in the first density gradient solution (1.10 g/ml sucrose, 0.1 mM MgCl$_2$, 1 mM Tris–acetate, pH 7.4). Crude ROS were carefully overlayed on top of a three-step gradient (1.11, 1.13, and 1.15 g/ml sucrose with 0.1 mM MgCl$_2$, 1 mM Tris–acetate, pH 7.4) and centrifuged at 85,000g for 30 min. The interface containing ROS was recovered, diluted with 0.01 mM Tris–acetate, pH 7.4, and ROS were pelleted again at 50,000g for 20 min. The pellet containing ROS was resuspended and stored at −80 °C prior to use in Western blot analyses.

2.4. Isolation of the ciliary apparatus by differential density gradient centrifugation

Isolation of ciliary apparati were performed as previously described (Fleischman, 1981; Horst, Forestner, & Besharse, 1987; Schmitt & Wolfrum, 2001; Wolfrum & Schmitt, 2000). Briefly, bovine retinas were isolated and kept at −80 °C. Frozen retinas were thawed in HBS buffer (115 mM NaCl, 2 mM KCl, 2 mM MgCl$_2$, 10 mM Hepes, pH 7), neuronal cells were cracked by gentle shaking for 1 min, filtered (400 μm, Millipore, Schwalbach, Germany) and enriched by a Sorvall RC-5B centrifuge, fixed angle rotor SS34, for 20 min at 4 °C and 48,000g. The pellet was resuspended in 50% sucrose (w/v), overlaid by HBS buffer and ultracentrifuged (Beckman-Coulter Optima max, rotor MLS 50) at 4 °C, 31,000g for 1 h. Cell fragments on the top of sucrose cushion were collected, added to a continuous sucrose gradient 25–50% and overlaid with buffer. After centrifugation for 2 h at 4 °C, 31,000g, two bands were collected. Probes were sedimented by decreasing the sucrose concentration. Pellets were resuspended in cytoskeleton extraction buffer (100 mM Hepes, 10 mM MgSO$_4$, 10 mM EGTA, 100 mM KCl, 5% DMSO, 20 mM DTT, 2% Triton X-100

adjusted to pH 7.5) and extracted on ice for 1 h. Ciliary apparati were separated by centrifugation for 3 h at 4 °C and 31,000g on a discontinuous sucrose gradient composed of 40, 50, and 60% (w/v) sucrose in a modified cytoskeleton extraction buffer (100 mM Hepes, 10 mM MgSO$_4$, 10 mM EGTA, 100 mM KCl).

2.5. Isolation of crude synaptosomes

Crude synaptosomes were prepared as described elsewhere (Hirao et al., 1998; Reiners et al., 2003). In brief, the brain of an adult mouse was homogenized in 800 μl extraction buffer (0.32 M sucrose in 4 mM Hepes, pH 7.4) and centrifuged at 800g for 10 min at 4 °C. The supernatant was centrifuged at 9200g for 15 min at 4 °C. The pellet was resuspended in 800 μl extraction buffer (0.32 M sucrose in 4 mM Hepes, pH 7.4) and centrifuged at 10,200g for 15 min at 4 °C. The crude synaptosome fraction was recovered in the pellet and resuspended in 800 μl buffer containing 20 mM Hepes/NaOH (pH 8.0), 100 mM NaCl, 5 mM EDTA, and 1% Triton X-100 and centrifuged at 100,000g for 30 min at 4 °C. The supernatant was used in Western blot analyses.

2.6. Serial tangential sectioning

Western blot analyses of serial tangential sections were performed as described by Reiners et al. (2003). Briefly, after removal of the vitreous, dissected rat eye cups were cut at four opposite sites and flat-mounted between two glass slides separated by 0.5 mm spacers. The bottom slide facing the basal membrane of the retina was roughened with sandpaper to improve adhesion. The top slide facing the outer side of the eye cup was covered with teflon spray to improve later release. The glass slide and eye cup sandwich was hold together by two small binder clips and frozen immediately on dry ice. The bottom slide with the eye cup was mounted into a cryomicrotome and sequential 10 μm tangential sections of the eye cups were collected in 100 μl SDS–PAGE sample buffer. Aliquots of 10 μl per lane were subjected to Western blot analyses.

2.7. Western blot analyses

For denaturing gel electrophoresis, the samples were mixed with SDS-PAGE sample buffer (62.5 mM Tris–HCl, pH 6.8; 10% glycerol; 2% SDS; 5% β-mercaptoethanol; 1 mM EDTA; 0.025% bromphenol blue). Twenty-five micrograms of protein extract per lane were separated on 12% polyacrylamide gels and transferred onto PVDF membranes (Millipore). Immunoreactivities were detected with the appropriate primary and corresponding secondary antibodies (IRDye 680 or 800, Rockland) employing the Odyssey infra red imaging system (LI-COR Biosciences, Lincoln, NE, USA). In case of the use of the ECL detection system (Amersham Biotech/ GE Healthcare, Freiburg, Germany) donkey anti-rabbit secondary antibodies coupled to horseradish peroxidase were applied to Western blot membranes. Band sizes were calculated using Total Lab software (Phoretics, UK). As a molecular marker a prestained ladder (Sigma–Aldrich), ranging from 11 to 170 kDa was used.

2.8. Immunofluorescence microscopy

Eyes from developing and adult mice were cryofixed directly in melting isopentane and cryosectioned as previously described (Wolfrum, 1991). Cryosections were placed on poly-L-lysine-precoated coverslips and incubated with 0.01% Tween 20 in PBS. PBS washed sections were blocked with blocking solution (0.5% cold water fish gelatin, 0.1% ovalbumin in PBS) for 30 min, and then incubated with primary antibodies in blocking solution overnight at 4 °C. Washed sections were subsequently incubated with secondary antibodies conjugated to Alexa 488 or Alexa 568 (Molecular Probes, Leiden, Netherlands) and DAPI (Sigma–Aldrich) for visualization of the nuclei, in blocking solution for 1–2 h at room temperature in the dark. After washing with PBS, sections were mounted in Mowiol 4.88 (Hoechst, Frankfurt, Germany). In none of the appropriate controls a reaction was observed. Mounted retinal sections were examined with a

Leica DMRB microscope (Leica microsystems, Bensheim, Germany). Images were obtained with a Hamamatsu ORCA ER CCD camera (Hamamatsu, Herrsching, Germany) and processed with Adobe Photoshop CS (Adobe Systems, San Jose, USA).

2.9. Cell culture

NIH3T3 cells were cultured in Dulbecco's modified Eagle's medium supplemented with 10% heat-inactivated fetal calf serum (FCS) and 2 mM glutamine. Immunofluorescence analyses were carried out on cells seeded on coverslips, followed by fixation with methanol and proceeded as previously described (Nagel-Wolfrum et al., 2004).

3. Results

3.1. Generation and validation of specific anti-SANS antibodies

Knowledge of expression profiles of proteins and their subcellular localization provide important insights in their specific function. So far, little was known about the expression and subcellular distribution of SANS. We generated a polyclonal antiserum against recombinant expressed murine SANS protein as a tool to study the expression and subcellular localization of SANS. Western blot analyses of

mouse retina extracts revealed that affinity purified anti-SANS antibodies decorated a band at approximately 55 kDa (Fig. 2A), corresponding to the predicted size of SANS (52 kDa). To validate the specificity of anti-SANS antibodies, Western blot analyses of extracts of mouse retina were performed with anti-SANS antibodies preadsorbed with the antigen used for immunization. The appropriate band for SANS was abolished (Fig. 2A), indicating the specificity of the anti-SANS antibodies. We further validated the specificity of the affinity purified antibodies on retinal cryosections (Fig. 2C–E). The specific SANS labeling described below was abolished when preadsorbed antibodies were applied to sections (Fig. 2E).

3.2. SANS protein is expressed in ciliated tissues

With these specific anti-SANS antibodies in hand, we analyzed the expression of SANS for the first time on protein level in various murine tissues (Fig. 3). Our Western blot analyses revealed SANS-specific bands of 55 kDa in protein extracts of the retina, the cochlea, the brain, the lung, the testis, the olfactory epithelium and of NIH3T3 cells. In addition to this 55 kDa band, a fade band at
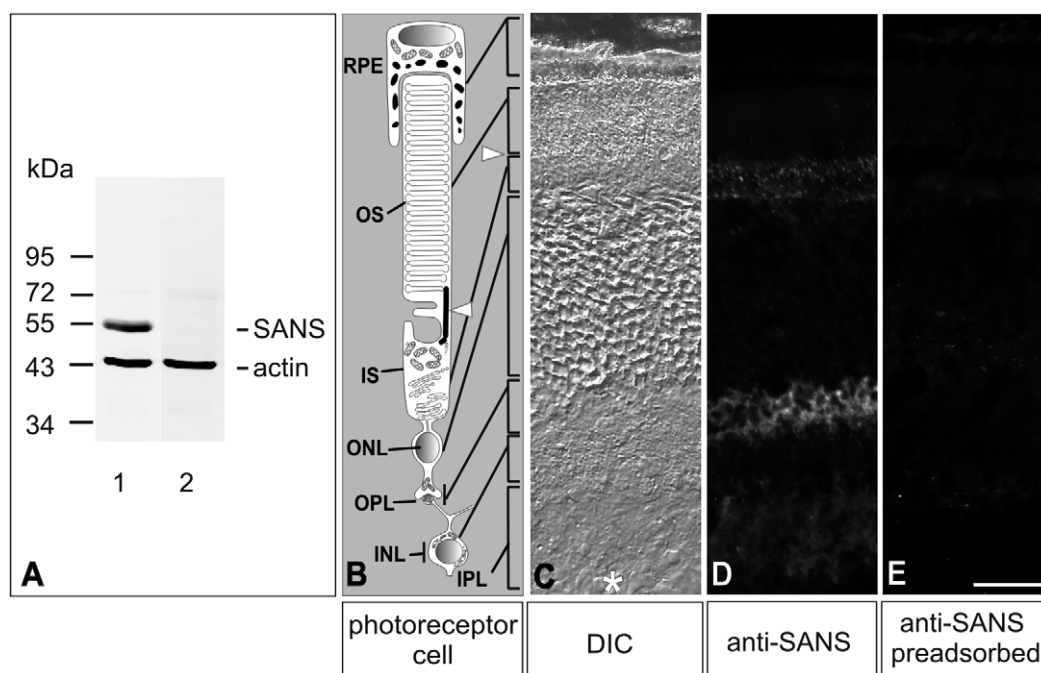
Fig. 2. Validation of anti-SANS antibodies by Western blot analyses and indirect immunofluorescence analyses of mouse retinas. (A) Western blot analysis of protein extract of mature mouse retina with affinity purified antibodies against SANS. A specific band with the molecular weight of approximately 55 kDa was obtained (lane 1). This band was completely abolished after preadsorption of anti-SANS antibodies with the corresponding antigen (lane 2). Coincubation with anti-actin was used as a loading control. (B) Schematic representation of a vertebrate rod photoreceptor cell. Vertebrate photoreceptors are composed of distinct morphological and functional compartments. The photosensitive outer segment (OS) is connected by the connecting cilium (arrowheads) with the biosynthetic active inner segment (IS). The cell body is localized in the outer nuclear layer (ONL) and contains the nucleus (N) and the synaptic terminal in the outer plexiform layer (OPL) of the retina. (C) Differential interference contrast (DIC) image visualizing the different retinal layers. (D) Indirect immunofluorescence analysis of anti-SANS on a longitudinal cryosection through a mature mouse retina. Anti-SANS immunofluorescence was localized in the photoreceptor cell layer and in the plexiform layers. In photoreceptor cells, SANS was detected at the ciliary complex, in the inner segment, the outer limiting membrane and at synapses in the OPL. No labeling was observed in the retinal pigmented epithelium (RPE) and the ganglion cell layer (asterisk in C). (E) Parallel section to (C and D), incubated with preadsorbed anti-SANS antibodies. After preadsorption, anti-SANS staining was abolished. Scale bar: 20 μm.
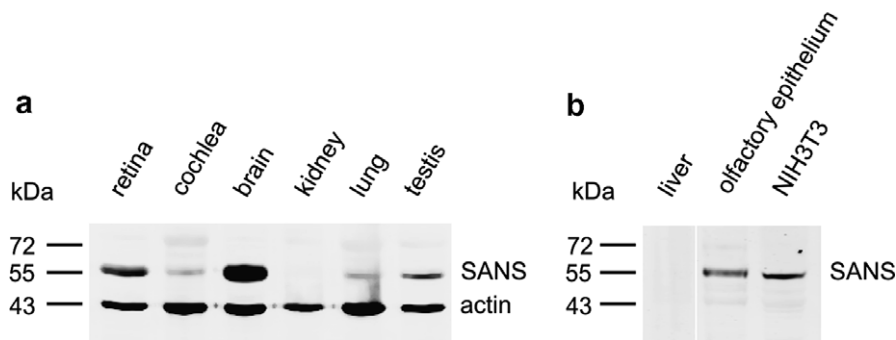
Fig. 3. SANS expression in murine ciliated tissues. (a and b) Western blot analyses of protein extracts of adult murine retina, cochlea, brain, kidney, lung, testis, liver, olfactory epithelium and NIH3T3 cells with anti-SANS antibodies. A specific band with a molecular weight of approximately 55 kDa was detected in NIH3T3 cells and in all analyzed tissues, apart from kidney and liver. The SANS-positive tissues contain ciliated cells. In the Western blots shown in (a), actin was used as loading control.

∼72 kDa was reproducible found in cochlea protein extracts. In contrast, no bands were obtained in kidney and liver tissue samples. In conclusion, our data indicate that the SANS protein is preferentially expressed in tissues containing ciliated cells.

3.3. SANS is localized in the photoreceptor cell layer, the inner plexiform layer and the outer plexiform layer of the mammalian retina

To determine the subcellular distribution of SANS in the retina, cryosections through mouse eyes were analyzed by immunofluorescence microscopy using affinity-purified anti-SANS antibodies. SANS expression was present in the photoreceptor cell layer, the outer limiting membrane, the inner plexiform layer and the outer plexiform layer of the retina (Fig. 2D). In contrast, no staining was observed in cells of the retinal pigmented epithelium (Fig. 2D). The same staining pattern by indirect immunofluorescence with anti-SANS antibodies were obtained in cryosections through the mature retina of other mammals, namely rats and pigs (data not shown). Furthermore, SANS expression was found in the photoreceptor cell layer, the outer limiting membrane and the plexiform layers of retinas of the amphibian *X. laevis* (data not shown).

3.4. SANS protein localization at the ciliary apparatus, the outer limiting membrane and the synapse of photoreceptor cells

To analyze the expression of SANS in photoreceptor cells immunohistochemical and biochemical analyses were performed. In a first set of experiments, the subcellular distribution of SANS was elucidated by immunohisto-chemistry of mature murine photoreceptors (Fig. 4). Immunofluorescence double labeling experiments with antibodies against SANS and marker proteins of subcellular compartments of photoreceptor cells were performed. Labeling with anti-pan-centrin antibodies (marker for the connecting cilium and basal body complex; Gießl et al., 2004) and anti-SANS antibodies revealed partial colocalization (Fig. 4A–C). This indicated SANS as a component of the connecting cilium and of the basal body complex. Furthermore, SANS was colocalized with β-catenin, a marker for the cell–cell adhesion in the inner segment at the outer limiting membrane (Golenhofen & Drenckhahn, 2000; Mehalow et al., 2003; Montonen, Aho, Uitto, & Aho, 2001) (Fig. 4D–F). In addition, antibodies against PSD-95 were applied. Although, PSD-95 is ubiquitously found in the post-synaptic dense differentiations (Kornau, Seeburg, & Kennedy, 1997), PSD-95 is known to be abundantly expressed in pre-synaptic terminals of photoreceptor cells (Koulen, Garner, & Wassle, 1998). Double labeling with anti-PSD-95 and anti-SANS antibodies revealed an overlapping staining pattern at synaptic terminals of photoreceptor cells (Fig. 4G–I). The obtained labeling for SANS was more distinct at the pre-synapse (Fig. 4G–I), indicating its localization in the synaptic terminal of rod and cone photoreceptor cells. A diminished localization for SANS was observed at post-synapses in second order neurons, in bipolar and horizontal cells.

3.5. SANS presence in subcellular fractionations of synaptosomes and photoreceptor cilia

To occlude the antigen masking occasionally observed in tissue sections we determined the subcellular localization of SANS in photoreceptor cells by Western blot analyses. Therefore, we carried out subcellular fractionations of photoreceptor cells and tangential cryosections through the rat retina. Western blot analyses revealed the presence of SANS in protein extracts of mouse and bovine retinas, in brain synaptosome fraction of mouse and in the ciliary fraction of bovine photoreceptor cells (Fig. 5a). However, in the fraction of isolated rod outer segments (ROS) a weak band was obtained which occurred most likely due to contamination of the ROS fraction with ciliary components. Differential density gradient centrifugation assays revealed that SANS was cosedimented with the ciliary marker acetylated α-tubulin (Fig. 5b).
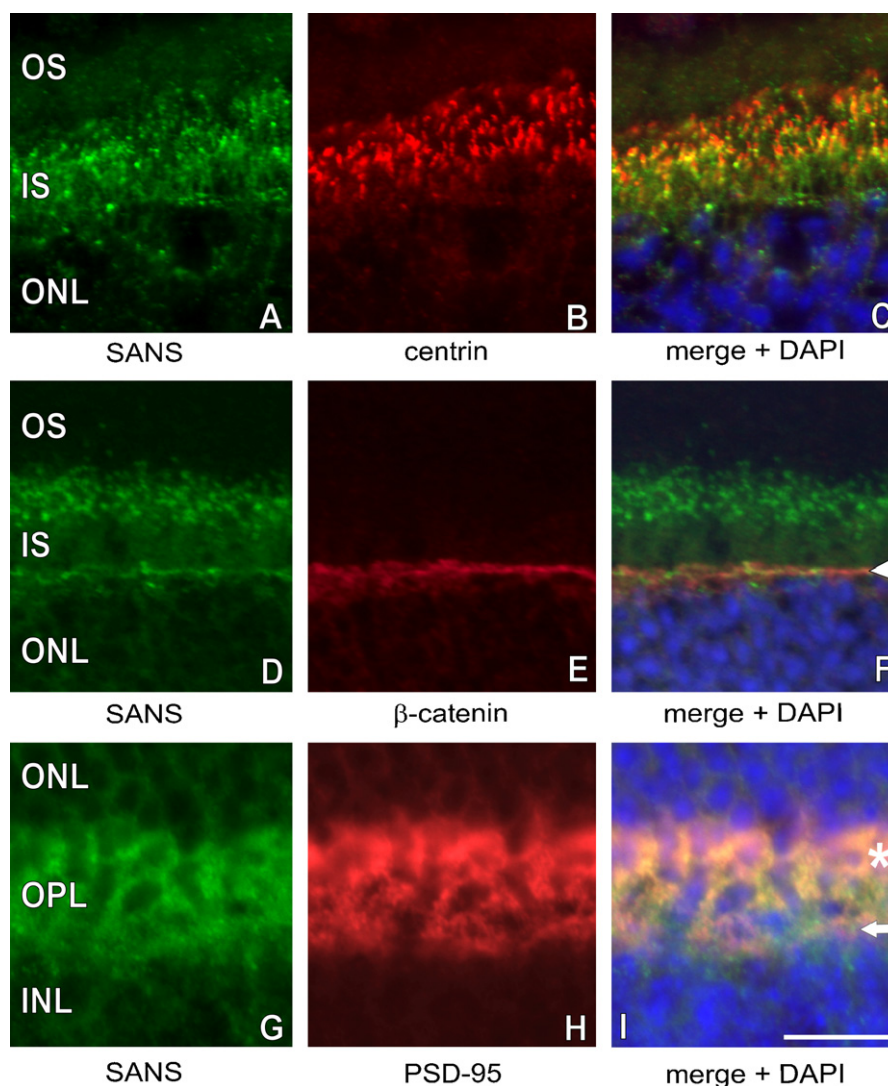
Fig. 4. Double labeling revealed SANS localization in the photoreceptor cilium, the outer limiting membrane and outer plexiform synapses of murine retinas. (A–I) Indirect double immunofluorescence analyses of photoreceptor compartments in retinal cryosections. (A–C) Double labeling with anti-SANS (A) and anti-pan-centrin antibodies (B), a marker for the ciliary apparatus (connecting cilium and the basal body). (C) Merge image of SANS and centrin labeling superposed with the nuclear DNA staining by DAPI. SANS and centrin were partially colocalized in the ciliary apparatus of photoreceptor cells. (D–F) Double labeling of anti-SANS (D) and anti-β-catenin antibodies (E), a molecular marker for the outer limiting membrane. (F) Merge image of SANS and β-catenin labeling superposed with DAPI staining. SANS and β-catenin were colocalized at the outer limiting membrane (arrowhead). (G–I) Double labeling with anti-SANS (G) and anti-PSD-95 antibodies (H), a marker for post-synapses, also staining pre-synaptic terminals in retinas. (I) Merge image of SANS and PSD-95 labeling superposed with DAPI staining. SANS and PSD-95 staining was colocalized in the synaptic terminals of photoreceptor cells (asterisk) and partially overlaps in the post-synaptic region of 2nd order neurons (bipolar cells and horizontal cells) (arrow). Scale bar: 10 μm.

3.6. Analysis of serial tangential cryosections of the retina confirmed SANS localization in the ciliary apparatus and synapse of photoreceptor cells

To validate the localization of SANS in photoreceptor cells we analyzed the protein distribution in serial tangential cryosections through the rat retina by Western blot analyses. For this purpose, we used antibodies against opsin, cytochrome *c*, and synaptophysin as markers to distinguish between the subcellular photoreceptor compartments (Reiners et al., 2003). Our analyses revealed that SANS was localized in the synaptic region and the inner segment, whereas SANS was not detected in the anti-opsin positive outer segment sections (Fig. 5c). Since SANS bands were obtained in sections at the transition of the compartment markers for the inner segment and outer segment, we concluded the presence of SANS in the ciliary apparatus of photoreceptor cells. This conclusion was further supported by the present semi-quantification of SANS protein in serial tangential sections. For this purpose, the optical density of Western blot bands was ascertained. These analyses revealed that SANS was enriched in the ciliary region more than two fold in comparison to other sub-compartments of photoreceptor cells (Fig. 5d). The applied
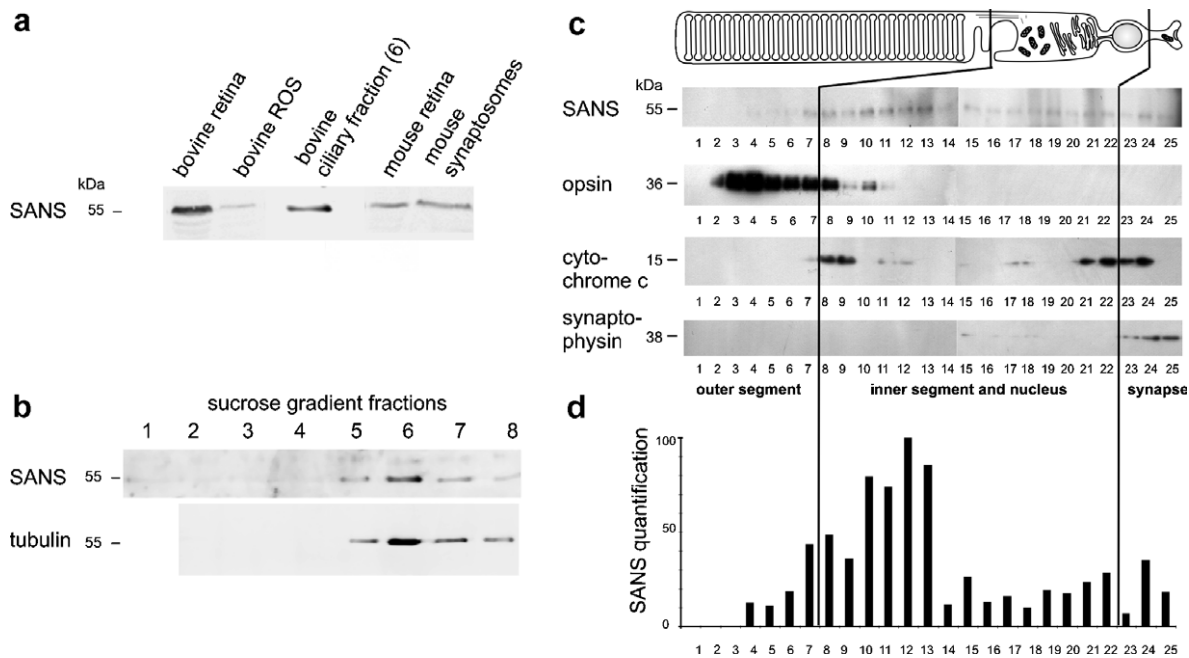
Fig. 5. Biochemical fractionations and analysis of serial tangential sections of retinas confirm SANS subcellular localization in photoreceptor cells. (a) Western blot analyses of subcellular fractions of mouse and bovine retinas. Prominent staining for SANS (~55 kDa) was present in total retina extract and the ciliary fraction of bovine photoreceptor cells (fraction 6 in b), whereas a weak band for SANS was obtained in rod outer segments (ROS). SANS was also detected in retina extract and in the synaptosome fraction of mice brain. (b) Western blot analyses of detergent-lysed bovine ciliary fractions harvested after differential gradient centrifugation. SANS cosediments with the ciliary marker acetylated α-tubulin. (c) Western blot analyses of tangential cryosections through a rat retina. Each lane corresponds to a 10 μm thick slice of the photoreceptor layer. Western blots with antibodies against opsin, cytochrome *c* and synaptophysin were used to determine the photoreceptor compartments assigning the outer segment, the inner segment and the synaptic region. SANS was detected in all tangential sections apart from anti-opsin positive slices of the outer segment. (d) SANS quantification by TotalLab software. The highest SANS protein concentration was present in sections at the transition of the compartment markers for the inner segment (marker: cytochrome *c*) and outer segment (marker: opsin)—the ciliary region of photoreceptor cells.

independent methods confirmed our previous immunohistochemical localization of SANS in the ciliary apparatus and at the synaptic region of mammalian photoreceptor cells.

3.7. SANS protein expression during postnatal maturation of the murine retina

We analyzed the expression and localization of SANS during various developmental stages of postnatal murine retinas. The expression of SANS protein was detected by Western blot analyses in all selected postnatal stages, namely PN0, PN7, PN14, and PN20 (Fig. 6). In addition,
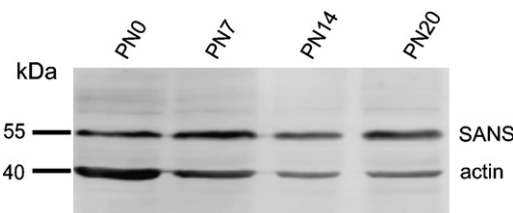
Fig. 6. SANS expression during postnatal differentiation of mouse retina. Western blot analyses with anti-SANS and anti-actin antibodies (loading control) of murine retina at different postnatal developmental stages, namely PN0, PN7, PN14, and PN20. SANS was detected at 55 kDa in all analyzed postnatal developmental stages.

we investigated the localization of SANS during retinal development by indirect immunofluorescence and DAPI counterstaining of the nuclear DNA (Fig. 7). Longitudinal sections of PN0 mouse eyes revealed SANS expression at the most apical tip of the neuroblast layer proximal to the retinal pigmented epithelium (Fig. 7A and E). Double labeling with anti-pan-centrin antibodies identified the punctuated anti-SANS stained structures as centrioles and basal bodies in photoreceptor precursors (Fig. 7I and M). The labeling of the differentiating ciliary apparatus of photoreceptor cells persists during all following developmental stages investigated (Fig. 7A–P). In the outer plexiform layer anti-SANS immunofluorescence was observed from PN14 on (Fig. 7C/G and D/H). At this retinal developmental stage synapses are formed in the outer plexiform layer in the mouse retina. SANS was localized at the cell–cell adhesion of the outer limiting membrane not before PN20 (Fig. 7D/H and L/P), when the mouse retina is fully maturated (von Kriegstein & Schmitz, 2003).

3.8. SANS localization at centrosomes and spindle poles of NIH3T3 cells

Our Western blot analyses revealed SANS expression in NIH3T3 fibroblasts. This prompted us to analyze the sub-
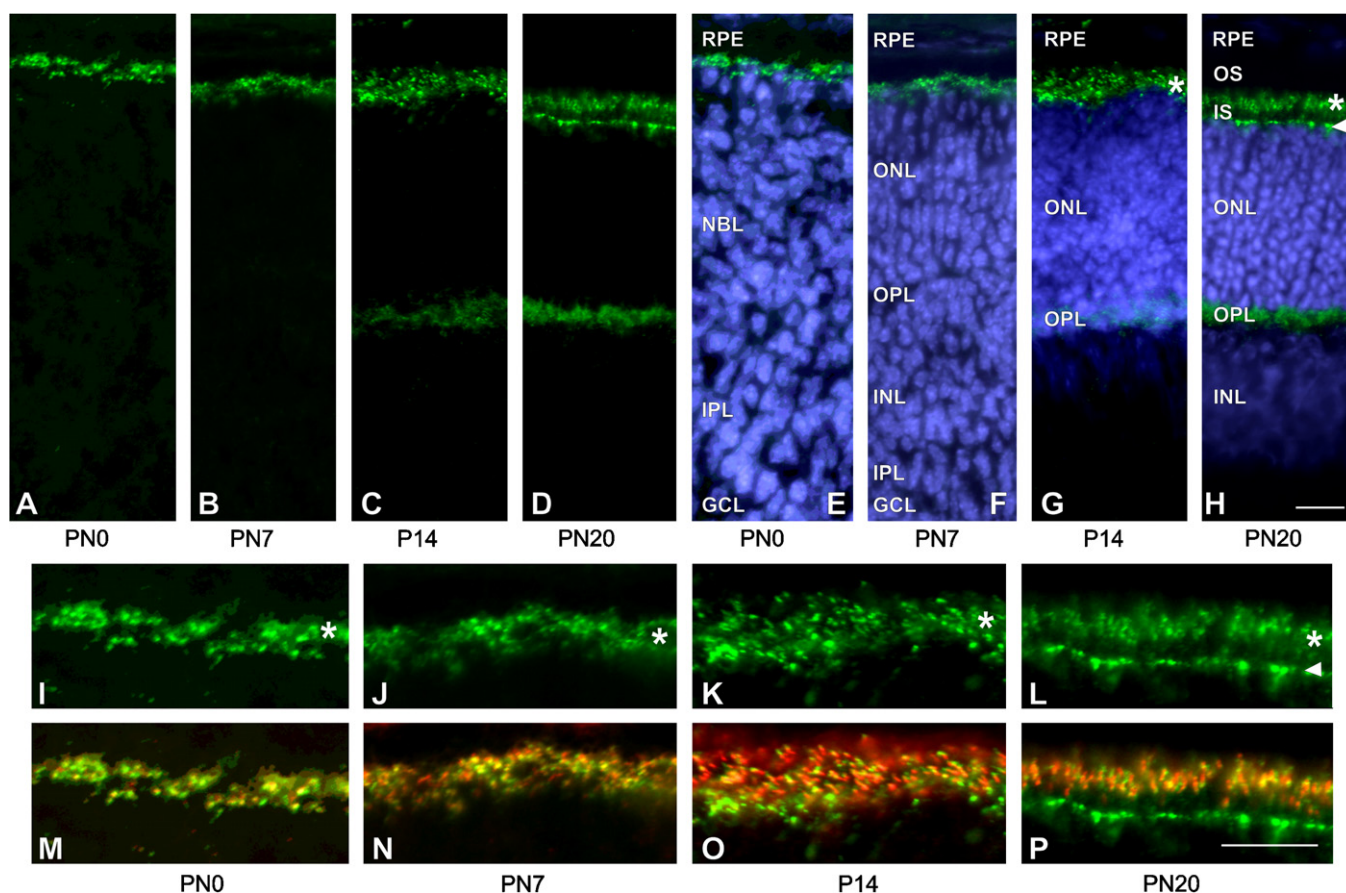
Fig. 7. SANS expression in photoreceptor cells of the maturing retina. (A–H) Indirect immunofluorescence with anti-SANS antibodies in cryosections through mouse retinas at different developmental stages. (E–H) Different nuclear layers in the developing retina were identified by counterstaining with DAPI. (A and E) In the PN0 retina, only the retinal pigmented epithelium (RPE), neuroblast layer (NBL), inner plexiform layer (IPL) and ganglion cell layer (GCL) are distinguishable. SANS labeling showed a punctuated staining pattern in the apical part of the developing retina, beneath the RPE cells. (B and F) In PN7, the neuroblast layer (NBL) is already divided in outer nuclear layer (ONL), the outer plexiform layer (OPL) and the inner nuclear layer (INL). Punctuated SANS staining was visible proximal to the RPE. (C and G) In PN14 eyes, SANS was localized in the ciliary region of photoreceptor cells (asterisk) and in the OPL, where synapses are differentiated. (D and H) In PN20 eyes, SANS labeling was localized at the ciliary region of photoreceptor cells (asterisk), in the OPL and in a thin line underneath the inner segment (IS), representing the outer limiting membrane (arrowhead). Outer segment = OS. (I–P) High magnification analyses of double immunofluorescence of ciliary regions (asterisks) in diverse developmental stages of murine photoreceptor cells shown in (A–H). (I–L) Indirect immunofluorescence of anti-SANS antibodies (green). (M–P) Merged images of anti-SANS (green) and anti-pan-centrin antibodies (red; a frequently used marker for centrioles, basal bodies and cilia of vertebrate photoreceptor cells). (I and M) In PN0 retinas, SANS was partially colocalized with centrins in basal bodies as soon as these are formed, beneath the apical membrane of photoreceptor precursor cells. (J and N) In PN7, SANS labeling revealed partial overlap with centrins in basal bodies and ciliary sprouts present in differentiating photoreceptor cells at this developmental stage. (K and O) In PN14, SANS was partially colocalized with centrins in basal bodies and the developing connecting cilium. (L and P) In PN20, SANS was partially colocalized with centrins in basal bodies and the connecting cilium. In addition, SANS was stained at the outer limiting membrane (arrowhead), which was not stained with anti-pan-centrin antibodies. Scale bars: 10 μm. (For interpretation of the references to the color in this figure legend the reader is referred to the web version of this article.)

cellular localization of SANS in cultured NIH3T3 fibroblasts to gain insight whether SANS has in addition an impact in non specialized cell types. Indirect immunofluorescence microscopy revealed partial colocalization of SANS with the centrosomal marker γ-tubulin at the centrosome of interphase cells (Fig. 8B and D). Further indirect immunocytochemical analyses of mitotic cells indicated that SANS was located at spindle pole bodies, essential for proper cell division (Fig. 8F and G). The obtained data point towards a general function of SANS at centrosome related structures, like basal bodies of cilia or centrioles.

4. Discussion

Recent studies indicated that SANS functions as a scaffold in the USH protein interactome (Adato et al., 2005; Weil et al., 2003; summarized in: Reiners et al., 2006; Kremer et al., 2006). So far, besides SANS homomer formation, interactions with harmonin isoforms a and b (USH1C), myosin VIIa (USH1B), and whirlin (USH2D) have been demonstrated (Adato et al., 2005; van Wijk et al., 2006; Weil et al., 2003; Maerker et al., 2007).

In the present study, we demonstrate that SANS protein expression is not restricted to the tissues mainly affected by
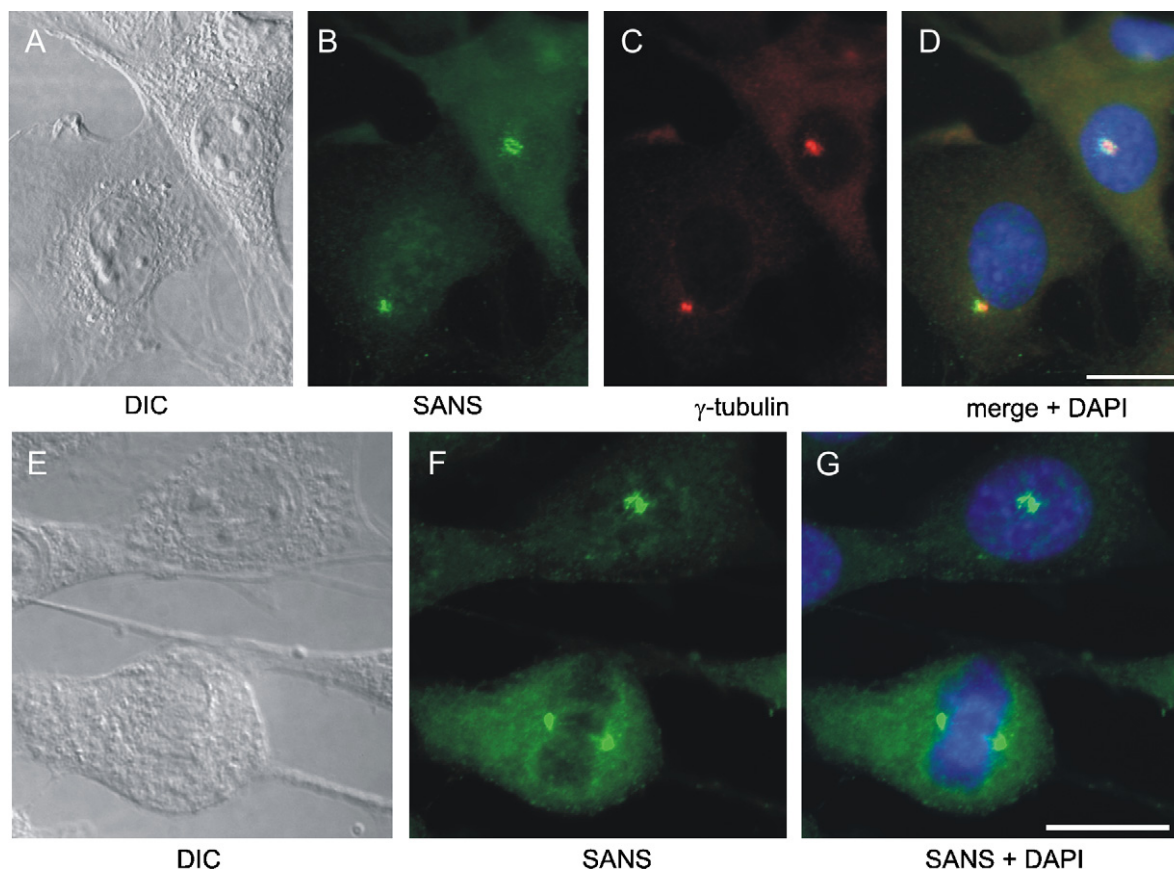
Fig. 8. SANS localization at centrosomes and spindle poles of NIH3T3 cells. (A–D) Double labeling of SANS (B) and γ-tubulin (C) in NIH3T3 cells by indirect immunofluorescence. (A) Differential interference contrast (DIC) image. (B) SANS staining was present throughout the cytoplasm and concentrated in a perinuclear spot. (C) Anti-γ-tubulin antibodies stained centrosomes. (D) Merged immunofluorescence images demonstrated partial colocalization of SANS and γ-tubulin at centrosomes. Nuclear DNA was stained with DAPI. (E–G) Localization of SANS in dividing NIH3T3 cells. (E) Differential interference contrast image. (F) SANS immunofluorescence analysis revealed SANS localization at spindle poles of dividing NIH3T3 cells. (G) Double labeling with anti-SANS antibodies and DAPI. Scale bar: 10 μm.

USH, the retina and inner ear. Western blot analyses revealed SANS specific bands at 55 kDa in further tissues, namely the brain, the lung, the testis and in the olfactory epithelium. Interestingly, we also obtained a band at ~72 kDa in protein extracts of cochleae. So far, we do not know the nature of this protein band. It may result from unspecific cross reactivity of the affinity purified anti-SANS antibody restricted to the cochlea protein extracts. Or, the band may represent the labeling of a higher molecular splice variant of SANS. Such alternatively spliced isoforms are well known from other USH proteins (Kremer et al., 2006; Petit, 2001; Reiners et al., 2006). Nevertheless, the obtained results for SANS protein expression correlate to previous mRNA expression analyses by RT-PCR (Johnston et al., 2004; Weil et al., 2003). All SANS positive tissues have the presence of ciliated cells in common. In SANS negative tissues, kidney and liver which also contain cells with primary cilia the expression of the SANS homologous Harp (harmonin-interacting, ankyrin repeat-containing protein) was shown (Johnston et al., 2004). Thus, Harp may resume the functional role of SANS in these tissues.

The tissue expression of the SANS protein is in line with the rather wide expression profile of other USH1 and 2 proteins (reviewed in: Reiners et al., 2006). This is in agreement with several studies on USH patients which indicate that USH can also affect other tissues, namely brain areas, olfactory and tracheal epithelia as well as sperm cells (see overview in: (Reiners et al., 2006). Such studies gathered histopathological data from USH patients displaying ciliary abnormalities not only in photoreceptor cells but also in olfactory epithelium and sperms. Based on these observations it has been suggested that USH is related to ciliary dysfunction (Arden & Fox, 1979), which is supported by the present study. SANS protein expression in tissues containing ciliated cells indicates that the pathophysiology of USH1G may also encroach cilia in cells of these tissues.

Our data show that SANS is expressed in the photoreceptor cell layer, the inner plexiform layer and the outer plexiform layer of the mammalian retina. Applied subcellular biochemical fractionations and immunological approaches determined the subcellular localization of SANS in photoreceptor cells at the ciliary apparatus and the synapse as well as at adhesion complexes of the outer

limiting membrane. Immunofluorescence analyses revealed that SANS was colocalized with markers for these subcellular photoreceptor compartments. Latter data were confirmed by results achieved by Western blot analyses of tangential cryosections. Furthermore, the localization of SANS in the ciliary apparatus and at the synapse of photoreceptor cells was corroborated by the enrichment of SANS in fractions of these compartments obtained by sucrose density gradient centrifugation. In all analyzed subcellular compartments of photoreceptor cells, networks of USH proteins were previously described (reviewed in: (Reiners et al., 2006). SANS may function as an integral component of these USH protein networks in diverse photoreceptor compartments. The integration of SANS in the USH protein interactome is shown in a schematic representation in Fig. 1b. The functional relevance of compartment specific interactions of SANS with its partner proteins will be discussed in the following paragraphs.

The ciliary apparatus of photoreceptor cells consists of a basal body complex from which the non-motile connecting cilium originates (reviewed in: (Besharse & Horst, 1990; Roepman & Wolfrum, 2007). The connecting cilium is placed in a strategic position at the joint between the inner segment and the outer segment of the photoreceptor cell. All exchanges between the inner and outer segment occur through the narrow and slender connecting cilium (Wolfrum, 1995). Currently, two in principle different alternative mechanisms of active transport through the connecting cilium towards the photoreceptor outer segment are discussed (Williams, 2002; Roepman & Wolfrum, 2007): (i) A microtubule-based translocation mediated by kinesin II associated with intraflagellar transport (IFT) complexes (Marszalek et al., 2000; Rosenbaum & Witman, 2002). (ii) Previous studies indicated that the USH network protein myosin VIIa (USH1B) is capable to transport cargo along actin filaments within the ciliary membrane (Liu, Udovichenko, Brown, Steel, & Williams, 1999; Wolfrum & Schmitt, 2000; Maerker et al., 2007; present study). In both alternative transport mechanisms SANS may participate. We have previously shown that SANS directly interacts with myosin VIIa (Adato et al., 2005). Similar localization of both proteins in the connecting cilium (Liu, Vansant, Udovichenko, Wolfrum, & Williams, 1997; Wolfrum & Schmitt, 2000) indicates that these interactions may take place within the ciliary compartment of photoreceptor cells. In this protein complex, SANS may provide the linkage to the prominent microtubule cytoskeleton of the cilium. An association of SANS with microtubules has been previously discussed (Adato et al., 2005; Roepman & Wolfrum, 2007). This is further supported by present results on SANS localization at microtubule organization centers, namely centrosomes and spindle poles in NIH3T3 cells and by a recent study by Maerker et al. (2007).

However, the integration of SANS into a ciliary USH protein network linked by myosin VIIa to actin filaments does not exclude an involvement of SANS in processes related to IFT complexes predominantly associated with microtubules. In photoreceptor cells, SANS and IFT proteins were both detected in the connecting cilium and in the basal body region (present study; Pazour et al., 2002; Maerker et al., 2007). In the basal body region, IFT proteins are thought to recruit cargo from inner segment transport carriers for the transport route through the connecting cilium (Pazour et al., 2002). SANS may also participate in processes of cargo handover between inner segment transport and the delivery through the connecting cilium (Maerker et al., 2007). A role for SANS in the transport of vesicles in inner ear hair cells has been previously suggested, where SANS was found in the periphery of the cuticular plate and in the basal body complex of the kinocilium of outer hair cells (Adato et al., 2005).

Our present study revealed that SANS is not only associated with the cilium of adult photoreceptor cells, but also during maturation of photoreceptor cells. During developmental stages PN0 and PN7, SANS was exclusively present at the apical tip of the neuroblast layer. During this time period ciliogenesis proceeds, basal bodies (centrioles) are placed in the apical inner segments and ciliary sprouts are formed at the photoreceptor apices (Uga & Smelser, 1973; Woodford & Blanks, 1989). Present double immunofluorescence analyses of SANS and centrins indicate that SANS is localized in basal bodies and growing cilia of maturing photoreceptor cells. This is in agreement with an association of SANS with the basal body complex of the kinocilium in differentiating outer hair cells of the inner ear (Adato et al., 2005). The presence of SANS in basal bodies of ciliated cells in tissues is further strengthened by the localization of SANS at the centrosomes and spindle poles of NIH3T3 cells. In general, basal bodies from which cilia arise are homologous to the mother centriole of centrosomes (Dawe, Farr, & Gull, 2007).

The present study revealed the localization of SANS at the outer limiting membrane also known as the *membrana limitans externa* (Spitznas, 1970). The outer limiting membrane is a layer of cell–cell adhesion contacts, mechanically strengthening the adhesion between photoreceptor cells and Mueller glia cells. Previous studies indicated that besides SANS other USH proteins are present in the outer limiting membrane (Ahmed et al., 2003; Reiners, Marker, et al., 2005; van Wijk et al., 2006). Homo- or heterophilic interaction of the ectodomains of protocadherin 15 (USH1F), cadherin 23 (USH1D), USH2A isoform b, and VLGR1b (USH2C) are thought to design connectors between the adjacent membranes of photoreceptor cells and Mueller glia cells. These contacts may be facilitated through intracellular tether of their cytoplasmic domains by parallel direct binding to the PDZ domains 1 and 2 of the scaffold protein whirlin (USH2D) (van Wijk et al., 2006). The direct interaction of SANS with whirlin may provide a conjunction of this protein network at the outer limiting membrane to microtubules.

Recently, we described the direct interaction of whirlin with MPP1, a membrane associated guanylate kinase

(MAGUK) protein of the large Crumbs protein complex at the outer limiting membrane (Gosens et al., 2007). Therefore, the USH protein network at the outer limiting membrane may be part of this multiprotein complex mainly organized by Crumbs1 and MPP5 (Gosens et al., 2007; Kantardzhieva et al., 2005). This complex is thought to serve in cell polarity and cell adhesion processes that are intimately connected and governs the formation and maintenance of the layered structure of vertebrate retina (Gosens et al., 2007; Kantardzhieva et al., 2005). The identified USH proteins may contribute to the function of the specialized Crumbs protein cell–cell adhesion complex at the outer limiting membrane. In conclusion, SANS may fulfill a role in bridging this cell–cell adhesion complex to the microtubule cytoskeleton and may participate in transport processes, necessary for the development and maintenance of the outer limiting membrane.

Our previous studies demonstrated localization of all identified USH1 and 2 proteins at photoreceptor and hair cell synapses (Reiners, van Wijk, et al., 2005, Reiners et al., 2006; van Wijk et al., 2006). Here, we confirm SANS as a further molecular component of the ribbon synapse of rod and cone photoreceptor cells. Present studies of developmental stages of the murine retina revealed that SANS protein expression was not found until PN14 when the synaptogenesis of ribbon synapses is terminated (von Kriegstein & Schmitz, 2003). Since our present data did not cover all stages during the critical period of synaptogenesis, we can not state whether or not SANS participates in the latter process. However, our data strengthen that SANS is part of the USH protein network present at the synapse in mature photoreceptor cells (reviewed in (Reiners et al., 2006). The current data set indicates that the PDZ domain containing USH scaffold proteins, harmonin and whirlin target the network components to the specialized ribbon synapses and tether their physiologic function there (Reiners et al., 2003, Reiners, van Wijk, et al., 2005; van Wijk et al., 2006). In the pre- and post-synaptic membrane of specialized photoreceptor synapses USH cadherins, cadherin 23, and protocadherin 15, as well as the transmembrane proteins USH2A and VLGR1b are thought to interact via their extracellular domains and keep the synaptic membranes in spatial proximity (Reiners et al., 2006). As in synapses in general, cytoplasmic scaffold proteins may anchor these adhesion molecules, but also transmembrane proteins as well as channels and receptors into the synaptic membrane (Garner, Nash, & Huganir, 2000). Our present results suggest that SANS is also part of this scaffolding machinery in ribbon synapses. By direct binding to the USH proteins harmonin, whirlin and myosin VIIa (see Fig. 1b) (Adato et al., 2005; van Wijk et al., 2006), SANS may connect the synaptic USH protein network with the microtubule cytoskeleton. However, in this association with microtubules, SANS may also participate in synaptic molecule trafficking and serve in the molecular handover from the long range microtubule-based neuronal transport system to the actin filament associated short

range transport system of the synaptic terminal, probably governed by the actin-based molecular motor myosin VIIa.

In conclusion, the scaffold protein SANS is a crucial component of photoreceptor cells involved in various structural and developmental processes associated with the microtubule cytoskeleton. Our data indicate that SANS participates in ciliogenesis during outer segment differentiation, in formation and maintenance of retina and photoreceptor cell polarity and in functions in the ribbon synapse of photoreceptor cells. For its essential specific functions SANS is integrated in protein networks in the ciliary apparatus, the outer limiting membrane and the ribbon synapse of photoreceptor cells. Defects of SANS may cause dysfunctions of entire USH protein networks and may lead overall to degeneration of the sensory systems in the inner ear and retina, symptoms characteristic for USH patients.

References

Adamus, G., Arendt, A., Zam, Z. S., McDowell, J. H., & Hargrave, P. A. (1988). Use of peptides to select for anti-rhodopsin antibodies with desired amino acid sequence specificities. *Peptide Research, 1*, 42–47.

Adamus, G., Zam, Z. S., Arendt, A., Palczewski, K., McDowell, J. H., & Hargrave, P. A. (1991). Anti-rhodopsin monoclonal antibodies of defined specificity: characterization and application. *Vision Research, 31*, 17–31.

Adato, A., Michel, V., Kikkawa, Y., Reiners, J., Alagramam, K. N., Weil, D., et al. (2005). Interactions in the network of Usher syndrome type 1 proteins. *Human Molecular Genetics, 14*, 347–356.

Ahmed, Z. M., Riazuddin, S., Riazuddin, S., & Wilcox, E. R. (2003). The molecular genetics of Usher syndrome. *Clinical Genetics, 63*, 431–444.

Arden, G. B., & Fox, B. (1979). Increased incidence of abnormal nasal cilia in patients with Retinitis pigmentosa. *Nature, 279*, 534–536.

Besharse, J. C., & Horst, C. J. (1990). The photoreceptor connecting cilium—a model for the transition zone. In R. A. Bloodgood (Ed.), *Ciliary and flagellar membranes* (pp. 389–417). New York: Plenum.

Boeda, B., El-Amraoui, A., Bahloul, A., Goodyear, R., Daviet, L., Blanchard, S., et al. (2002). Myosin VIIa, harmonin and cadherin 23, three Usher 1 gene products that cooperate to shape the sensory hair cell bundle. *EMBO Journal, 21*, 6689–6699.

Dawe, H. R., Farr, H., & Gull, K. (2007). Centriole/basal body morphogenesis and migration during ciliogenesis in animal cells. *Journal of Cell Science, 120*, 7–15.

Davenport, S. L. H., Omenn, G. S., (1977). The heterogeneity of Usher syndrome. *Fifth international conference on birth defects*, Montreal.

Ebermann, I., Scholl, H. P., Charbel, I. P., Becirovic, E., Lamprecht, J., Jurklies, B., et al. (2007). A novel gene for Usher syndrome type 2: Mutations in the long isoform of whirlin are associated with retinitis pigmentosa and sensorineural hearing loss. *Human Genetics, 121*, 203–211.

Fleischman, D. (1981). Rod guanylate cyclase located in axonemes. *Current Topics in Membranes and Transport, 15*, 109–119.

Garner, C. C., Nash, J., & Huganir, R. L. (2000). PDZ domains in synapse assembly and signalling. *Trends in Cell Biology, 10*, 274–280.

Gießl, A., Pulvermüller, A., Trojan, P., Park, J. H., Choe, H.-W., Ernst, O. P., et al. (2004). Differential expression and interaction with the visual G-protein transducin of centrin isoforms in mammalian photoreceptor cells. *Journal of Biological Chemistry, 279*, 51472–51481.

Golenhofen, N., & Drenckhahn, D. (2000). The catenin, p120ctn, is a common membrane-associated protein in various epithelial and non-epithelial cells and tissues. *Histochemistry and Cell Biology, 114*, 147–155.

Gosens, I., van Wijk, E., Kersten, F. F., Krieger, E., van der, Z. B., Marker, T., et al. (2007). MPP1 links the Usher protein network and the Crumbs protein complex in the retina. *Human Molecular Genetics*, Epub ahead of print.

Hirao, K., Hata, Y., Ide, N., Takeuchi, M., Irie, M., Yao, I., et al. (1998). A novel multiple PDZ-domain-containing molecule interacting with *N*-methyl-D-aspartate receptors and neuronal cell adhesion proteins. *Journal of Biological Chemistry, 273*, 21105–21110.

Horst, C. J., Forestner, D. M., & Besharse, J. C. (1987). Cytoskeletal-membrane interactions: Between cell surface glycoconjugates and doublet microtubules of the photoreceptor connecting cilium. *Journal of Cell Biology, 105*, 2973–2987.

Johnston, A. M., Naselli, G., Niwa, H., Brodnicki, T., Harrison, L. C., & Gonez, L. J. (2004). Harp (harmonin-interacting, ankyrin repeat-containing protein), a novel protein that interacts with harmonin in epithelial tissues. *Genes to Cells, 9*, 967–982.

Kantardzhieva, A., Gosens, I., Alexeeva, S., Punte, I. M., Versteeg, I., Krieger, E., et al. (2005). MPP5 recruits MPP4 to the CRB1 complex in photoreceptors. *Investigative Ophthalmology & Visual Science, 46*, 2192–2201.

Kikkawa, Y., Shitara, H., Wakana, S., Kohara, Y., Takada, T., Okamoto, M., et al. (2003). Mutations in a new scaffold protein Sans cause deafness in Jackson shaker mice. *Human Molecular Genetics, 12*, 453–461.

Kornau, H. C., Seeburg, P. H., & Kennedy, M. B. (1997). Interaction of ion channels and receptors with PDZ domain proteins. *Current Opinion in Neurobiology, 7*, 368–373.

Koulen, P., Garner, C. C., & Wassle, H. (1998). Immunocytochemical localization of the synapse-associated protein SAP102 in the rat retina. *Journal of Comparative Neurology, 397*, 326–336.

Kremer, H., van Wijk, E., Märker, T., Wolfrum, U., & Roepman, R. (2006). Usher syndrome: Molecular links of pathogenesis, proteins and pathways. *Human Molecular Genetics, 15*(Suppl. 2), R262–R270.

Liu, X., Udovichenko, I. P., Brown, S. D., Steel, K. P., & Williams, D. S. (1999). Myosin VIIa participates in opsin transport through the photoreceptor cilium. *Journal of Neuroscience, 19*, 6267–6274.

Liu, X. R., Vansant, G., Udovichenko, I. P., Wolfrum, U., & Williams, D. S. (1997). Myosin VIIa, the product of the Usher 1B syndrome gene, is concentrated in the connecting cilia of photoreceptor cells. *Cell Motility and the Cytoskeleton, 37*, 240–252.

Marszalek, J. R., Liu, X., Roberts, E. A., Chui, D., Marth, J. D., Williams, D. S., et al. (2000). Genetic evidence for selective transport of opsin and arrestin by kinesin-II in mammalian photoreceptors. *Cell, 102*, 175–187.

Maerker, T., van Wijk, E., Overlack, N., Kersten, F. F. J., McGee, J., Goldmann, T., et al. (2007). A novel Usher protein network at the periciliary reloading point between molecular transport machineries in vertebrate photoreceptor cells. *Human Molecular Genetics*, accepted for publication.

Mehalow, A. K., Kameya, S., Smith, R. S., Hawes, N. L., Denegre, J. M., Young, J. A., et al. (2003). CRB1 is essential for external limiting membrane integrity and photoreceptor morphogenesis in the mammalian retina. *Human Molecular Genetics, 12*, 2179–2189.

Montonen, O., Aho, M., Uitto, J., & Aho, S. (2001). Tissue distribution and cell type-specific expression of p120ctn isoforms. *Journal of Histochemistry & Cytochemistry, 49*, 1487–1496.

Nagel-Wolfrum, K., Buerger, C., Wittig, I., Butz, K., Hoppe-Seyler, F., & Groner, B. (2004). The interaction of specific peptide aptamers with the DNA binding domain and the dimerization domain of the transcription factor Stat3 inhibits transactivation and induces apoptosis in tumor cells. *Molecular Cancer Research, 2*, 170–182.

Nourry, C., Grant, S. G., & Borg, J. P. (2003). PDZ domain proteins: plug and play! *Science's STKE, 2003*, RE7.

Papermaster, D. S. (1982). Preparation of retinal rod outer segments. *Methods in Enzymology, 81*, 48–52.

Pazour, G. J., Baker, S. A., Deane, J. A., Cole, D. G., Dickert, B. L., Rosenbaum, J. L., et al. (2002). The intraflagellar transport protein, IFT88, is essential for vertebrate photoreceptor assembly and maintenance. *Journal of Cell Biology, 157*, 103–113.

Petit, C. (2001). Usher syndrome: From genetics to pathogenesis. *Annual Review of Genomics and Human Genetics, 2*, 271–297.

Pulvermüller, A., Gießl, A., Heck, M., Wottrich, R., Schmitt, A., Ernst, O. P., et al. (2002). Calcium dependent assembly of centrin/G-protein complex in photoreceptor cells. *Molecular and Cellular Biology, 22*, 2194–2203.

Reiners, J., Marker, T., Jurgens, K., Reidel, B., & Wolfrum, U. (2005). Photoreceptor expression of the Usher syndrome type 1 protein protocadherin 15 (USH1F) and its interaction with the scaffold protein harmonin (USH1C). *Molecular Vision, 11*, 347–355.

Reiners, J., van Wijk, E., Maerker, T., Zimmermann, U., Juergens, K., te Brinke, H., et al. (2005). Scaffold protein harmonin (USH1C) provides molecular links between Usher syndrome type 1 and type 2. *Human Molecular Genetics, 14*, 3933–3943.

Reiners, J., Nagel-Wolfrum, K., Jurgens, K., Marker, T., & Wolfrum, U. (2006). Molecular basis of human Usher syndrome: deciphering the meshes of the Usher protein network provides insights into the pathomechanisms of the Usher disease. *Experimental Eye Research, 83*, 97–119.

Reiners, J., Reidel, B., El-Amraoui, A., Boeda, B., Huber, I., Petit, C., et al. (2003). Differential distribution of harmonin isoforms and their possible role in Usher-1 protein complexes in mammalian photoreceptor cells. *Investigative Ophthalmology & Visual Science, 44*, 5006–5015.

Roepman, R., & Wolfrum, U. (2007). Protein networks and complexes in photoreceptor cilia. In E. Bertrand & M. Faupel (Eds.). *Subcellular proteomics from cell deconstruction to system reconstruction* (Vol. 43, pp. 209–235). New York: Springer, Chapter 10.

Rosenbaum, J. L., & Witman, G. B. (2002). Intraflagellar transport. *Nature Reviews. Molecular Cell Biology, 3*, 813–825.

Schmitt, A., & Wolfrum, U. (2001). Identification of novel molecular components of the photoreceptor connecting cilium by immunoscreens. *Experimental Eye Research, 73*, 837–849.

Sedgwick, S. G., & Smerdon, S. J. (1999). The ankyrin repeat: A diversity of interactions on a common structural framework. *Trends in Biochemical Sciences, 24*, 311–316.

Siemens, J., Kazmierczak, P., Reynolds, A., Sticker, M., Littlewood Evans, A., & Müller, U. (2002). The Usher syndrome proteins cadherin 23 and harmonin form a complex by means of PDZ-domain interactions. *Proceedings of the National Academy of Sciences of the United States of America, 99*, 14946–14951.

Spitznas, M. (1970). The fine structure of the so-called outer limiting membrane in the human retina. *Albrecht von Graefes Archin fur Klinische Experimentelle Ophthalmologie, 180*, 44–56.

Stapleton, D., Balan, I., Pawson, T., & Sicheri, F. (1999). The crystal structure of an Eph receptor SAM domain reveals a mechanism for modular dimerization. *Nature Structure Biology, 6*, 44–49.

Uga, S., & Smelser, G. K. (1973). Electron microscopic study of the development of retinal Mullerian cells. *Investigative Ophthalmology, 12*, 295–307.

van Wijk, E., van der Zwaag, B., Peters, T., Zimmermann, U., te Brinke, H., Kersten, F. F., et al. (2006). The DFNB31 gene product whirlin connects to the Usher protein network in the cochlea and retina by direct association with USH2A and VLGR1. *Human Molecular Genetics, 15*, 751–765.

von Kriegstein, K., & Schmitz, F. (2003). The expression pattern and assembly profile of synaptic membrane proteins in ribbon synapses of the developing mouse retina. *Cell and Tissue Research, 311*, 159–173.

Weil, D., El-Amraoui, A., Masmoudi, S., Mustapha, M., Kikkawa, Y., Lainé, S., et al. (2003). Usher syndrome type I G (USH1G) is caused by mutations in the gene encoding SANS, a protein that associates with the USH1C protein, harmonin. *Human Molecular Genetics, 12*, 463–471.

Williams, D. S. (2002). Transport to the photoreceptor outer segment by myosin VIIa and kinesin II. *Vision Research, 42*, 455–462.

Wolfrum, U. (1991). Tropomyosin is co-localized with the actin filaments of the scolopale in insect sensilla. *Cell and Tissue Research, 265*, 11–17.

Wolfrum, U. (1995). Centrin in the photoreceptor cells of mammalian retinae. *Cell Motility and the Cytoskeleton, 32*, 55–64.

Wolfrum, U., & Salisbury, J. L. (1998). Expression of centrin isoforms in the mammalian retina. *Experimental Cell Research, 242*, 10–17.

Wolfrum, U., & Schmitt, A. (2000). Rhodopsin transport in the membrane of the connecting cilium of mammalian photoreceptor cells. *Cell Motility and the Cytoskeleton, 46*, 95–107.

Woodford, B. J., & Blanks, J. C. (1989). Localization of actin and tubulin in developing and adult mammalian photoreceptors. *Cell and Tissue Research, 256*, 495–505.